NJC

Accepted Manuscript

This is an *Accepted Manuscript*, which has been through the Royal Society of Chemistry peer review process and has been accepted for publication.

Accepted Manuscripts are published online shortly after acceptance, before technical editing, formatting and proof reading. Using this free service, authors can make their results available to the community, in citable form, before we publish the edited article. We will replace this *Accepted Manuscript* with the edited and formatted *Advance Article* as soon as it is available.

You can find more information about *Accepted Manuscripts* in the Information for Authors.

Please note that technical editing may introduce minor changes to the text and/or graphics, which may alter content. The journal's standard Terms & Conditions and the Ethical guidelines still apply. In no event shall the Royal Society of Chemistry be held responsible for any errors or omissions in this *Accepted Manuscript* or any consequences arising from the use of any information it contains.

ROYAL SOCIETY OF CHEMISTRY

www.rsc.org/njc

New Journal of Chemistry RSCPublishing

ARTICLE

Highly efficient yellow phosphorescent OLEDs based on two novel bipolar host materials

Cite this: DOI: 10.1039/x0xx00000x

Song Zhang, Qiu-Lei Xu, Jing-Cheng Xia, Yi-Ming Jing, You-Xuan Zheng*, Jing-Lin Zuo

Received 00th January 2012,
Accepted 00th January 2012

DOI: 10.1039/x0xx00000x

www.rsc.org/

Two bipolar host materials, N^1-(naphthalen-1-yl)-N^1,N^4-diphenyl-N^4-(4-(5-phenyl-1,3,4-oxadiazol-2-yl)phenyl)naphthalene-1,4-diamine (**NONP**) and N^1-(naphthalen-1-yl)-N^1,N^4-diphenyl-N^4-(3-(5-phenyl-1,3,4-oxadiazol-2-yl)phenyl)naphthalene-1,4-diamine (**NONM**), comprising a hole-transporting N^1-(naphthalen-1-yl)-N^1,N^4-diphenylnaphthalene-1,4-diamine (**NPNA2**) donor and an electron-transporting 1,3,4-oxadiazole (**OXD**) acceptor at different positions of phenyl bridge have been synthesized. **NONP** (glass transition temperature T_g = 127 °C) and **NONM** (T_g = 105 °C) exhibit high morphological stability. The theoretical calculations of two hosts show that the HOMOs (highest occupied molecular orbitals) are mainly dispersed on the electron donating groups and LUMOs (lowest unoccupied molecular orbitals) are predominantly dispersed on the electron accepting units, respectively, suggesting bipolar charge transporting property. Two yellow phosphorescent organic light-emitting diodes (PHOLEDs, ITO (indium tin oxide) / TAPC (1,1-bis[4-(di-*p*-tolylamino) phenyl]cyclohexane, 40 nm)/ host: $Ir(bt)_2(acac)$ (bis(2-phenylbenzothiozolato-N,$C^{2'}$)iridium(acetylacetonate), 15 wt%, 20 nm)/ TmPyPB (1,3,5-tri(*m*-pyrid-3-yl-phenyl) benzene, 40 nm)/ LiF (1 nm)/ Al (100 nm)) fabricated using **NONP** and **NONM** as the host and $Ir(bt)_2(acac)$ as the emitter exhibit maximum current efficiencies ($\eta_{c,max}$) of 43.2 and 44.4 cd A^{-1}, respectively, with low current efficiency roll-off. The values of 40.4 and 43.6 cd A^{-1} are still can be achieved at the luminance of 3000 cd m^{-2}, respectively.

Introduction

In the last few years the organic light-emitting diodes (OLEDs) industry enjoyed fast growth, as OLEDs are widely considered to be the leading next-generation display and lighting technology. Among these devices, tremendous efforts have been made in the improvement of phosphorescent organic light emitting diodes (PHOLEDs) because they can reach 100% internal quantum efficiency by harvesting both electro-generated singlet and triplet excitons for emission.[1] The emissive layer of a PHOLED is usually doped with an organometallic complex, which contains heavy metal atoms (usually iridium). The interaction between the heavy metal and organic molecules can result in more efficient and longer lifetime emitters. However, the emission lifetime and high concentration of these heavy metal complexes are easy to lead to undesired efficiency roll-off at high current density during the operation of a device.[2] Therefore, to achieve highly efficient electrophosphorescence by reducing competitive factors such as concentration quenching and triplet-triplet annihilation, phosphorescent emitters of heavy-metal complexes are usually doped uniformly in an organic host material.[3] The design of appropriate host materials is of great importance for highly efficient OLEDs, and it should meet some basic requirements: (a) sufficiently high triplet energy (E_T) for ensuring exothermic energy transfer from the host material to the dopant and efficient exciton confinement,[4] (b) a high morphological stability (high glass transition temperature (T_g), especially), (c) suitable energy level match-ups with adjacent layers to reduce interfacial energy barriers,[5] (d) decent charge carrier transport properties to increase the opportunity for electron and hole recombination within the emitting layer.[6]

For OLEDs, if only one type of charge carrier is preferentially injected and transported, recombination of the opposite charges will be shifted out of the emissive layer, lowering the device efficiency.[7] Therefore, bipolar hosts have aroused considerable interests in the area of OLEDs because they can provide more balance in electron and hole fluxes and help increase the probability of carrier recombination.[8] A simple and viable strategy for designing

bipolar hosts is to simultaneously incorporate an electron donor (D) and electron acceptor (A) subunits in one molecular skeleton without lowering the E_T as the result of intramolecular charge transfer.[6] In this case, the introduction of twisted molecular conformation may be an efficient strategy to achieve high triplet energy.

The dimer of the *N*-phenyl-1-naphthylamine, N^1-(naphthalen-1-yl)-N^1,N^4-diphenylnaphthalene-1,4-diamine (**NPNA2**), has ever been characterized to have high triplet energy, excellent hole-transporting ability and high thermal stability.[9] And the 1,3,4-oxadiazole (**OXD**) derivatives are well established electron-transporting and hole-blocking materials used in OLEDs due to the electron-withdrawing nature of this aromatic heterocycle molecule.[10] In the case of that, the hole-transporting **NPNA2** and electron-transporting 1,3,4-oxadiazole moieties were selected for the construction of two new bipolar compounds (Scheme 1), N^1-(naphthalen-1-yl)-N^1,N^4-diphenyl-N^4-(4-(5-phenyl-1,3,4-oxadiazol-2-yl)phenyl) naphthalene-1,4-diamine (**NONP**) and N^1-(naphthalen-1-yl)-N^1,N^4-diphenyl-N^4-(3-(5-phenyl-1,3,4-oxadiazol-2-yl)phenyl) naphthalene-1,4-diamine (**NONM**), to study the effects of the positions of 1,3,4-oxadiazole on the phenyl bridge. As the yellow phosphors play the indispensable role to achieve high efficiencies in two-color, all-phosphor white organic light-emitting diodes, the yellow phosphor $Ir(bt)_2(acac)$ (bis(2-phenylbenzothiozolato-N,$C^{2'}$)iridium(acetylacetonate))[11] was chose as emitter in this study. And in our previous report, we fabricated devices with hosts connecting triphenylsilane, **NPNA2** moieties and $Ir(bt)_2(acac)$ as guest achieved maximum current efficiency of 40.8 cd A^{-1}.[12] But unfortunately, those materials are hole transport hosts. Therefore, we introduce the more electron deficient moiety **OXD** to develop the bipolar property of the hosts and expect to achieve higher efficiencies of PHOLEDs. The triplet energy levels of the two novel host materials are higher than $Ir(bt)_2(acac)$ and efficient energy transfer from the host materials to the $Ir(bt)_2(acac)$ is expected.

Results and discussion

Synthesis and thermal property

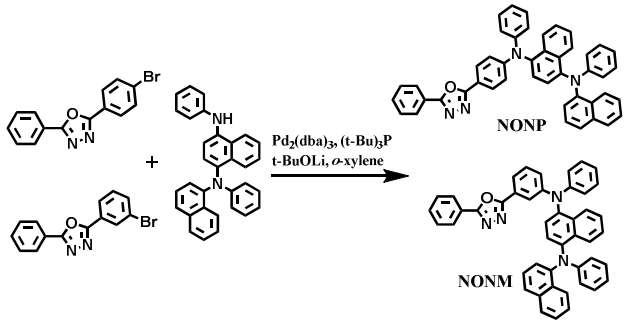

Scheme 1. Synthetic routes of **NONP** and **NONM**.

Scheme 1 shows the synthetic routes and structures of **NONP** and **NONM**. The starting material, 2-(4-bromophenyl)-5-phenyl-1,3,4-oxadiazole and 2-(3-bromophenyl)-5-phenyl-1,3,4-oxadiazole were synthesized from ring closing reaction of *N*-benzoyl-4-bromobenzohydrazide and *N*-benzoyl-4-bromobenzo hydrazide, respectively, which were prepared by hydrazinolysis of benzoyl chloride. N^1-(naphthalen-1-yl)-N^1,N^4-diphenyl naphthalene-1,4-diamine (**NPNA2**) was synthesized as reported previously.[9] Buchwald-Hartwig crossing-coupling of 2-(4-bromophenyl)-5-phenyl-1,3,4-oxadiazole and 2-(3-bromophenyl)-5-phenyl-1,3,4-oxadiazole with **NPNA2** gave **NONP** and **NONM** with yields higher than 60%.

The thermal properties of **NONP** and **NONM** were characterized by thermogravimetric analysis (TGA, Fig. 1) and differential scanning calorimetry (DSC, Fig. 1). TGA of **NONP** and **NONM** showed a decomposition temperature (T_d) corresponding to 5% weight loss as high as 424 ºC and 375 ºC, respectively. More importantly, high glass transition temperatures are observed in **NONP** (T_g = 127 °C) and **NONM** (T_g = 106 °C). This can be partly due to the molecular structures containing of the hole-transporting unit **NPNA2**, which increase molecular asymmetry and molecular weight. This demonstrated that two host materials are capable of forming uniform amorphous films, which are one of the key factors for highly efficient PHOLEDs.

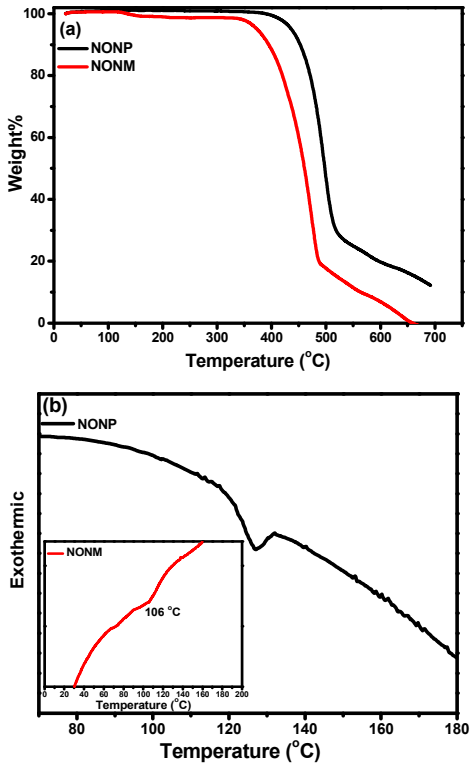

Fig. 1 TGA (a) and DSC (b) thermograms of **NONP** (black line) and **NONM** (red line).

Photophysical properties

Photophysical properties of **NONP** and **NONM** were examined by UV-vis and photoluminescence (PL) spectrometry (Fig. 2 and Table 1). The absorption spectra of **NONP**, **NONM** and $Ir(bt)_2(acac)$ were tested in dichloromethane solution. The two short-wavelength absorptions peaking at 268 and 276 nm in **NONP** and **NONM** can be attributed to the π-π* transitions from the electron-donating **NPNA2** moiety to the electron-accepting **OXD** unit (intramolecular charge transfer). The longer wavelength absorptions observed at 351 nm for **NONP** and 372 nm for **NONM** are attributed to the **NPNA2** centered n-π* transition. The absorption bands of $(bt)_2Ir(acac)$ at 441 and 481 nm are belong to the absorption transition from ground state to singlet ^{1}MLCT and triplet ^{3}MLCT excited state.[13]

Table 1. Photophysical data of compounds **NONP** and **NONM.**

Compound	T_d/T_g [a] (°C)	Absorption λ_{abs}(nm) [b]	Emission λ_{em}(nm) [b]	E_T [c] (eV)	τ [d] (ms)	HOMO (eV)	LUMO (eV)
NONP	424/127	268/351	444	2.71	1.2, 13.9	-5.27	-2.33
NONM	375/105	276/372	447	2.73	1.04, 14.8	-5.25	-2.30

[a] T_g: Glass transition temperatures, T_d: decomposition temperatures. [b] Measured in dichloromethane solution at 298 K. [c] Triplet energy: estimated from the highest-energy peaks of the 40 K phosphorescence spectra. [d] Measured in zeonex at 40 K, λ_{ex} = 380 nm.

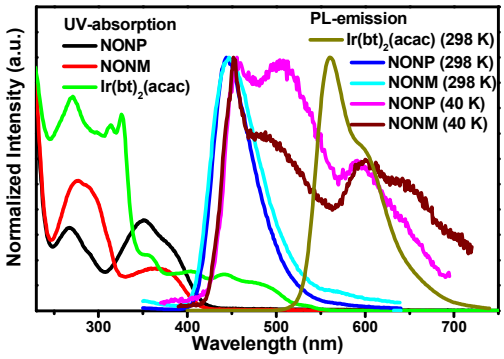

Fig. 2 UV-vis spectra of **NONP**, **NONM** and $Ir(bt)_2(acac)$ in dichloromethane solution at room temperature; photoluminescence spectra of **NONP**, **NONM** and $Ir(bt)_2(acac)$ in dichloromethane solution at 298 K; phosphorescence spectra of **NONP** and **NONM** at 40 K.

The fluorescence spectra of **NONP**, **NONM** and phosphorescence spectrum of $Ir(bt)_2(acac)$ at room temperature are also shown in Fig 2. The maximum emission peak of $Ir(bt)_2(acac)$ located at 560 nm with a slight shoulder at 597 nm. The emission peaks of **NONP** and **NONM** at room temperature are 444 and 447 nm, respectively. There is a good overlap between the emission bands of **NONP**, **NONM** and the MLCT absorption of $Ir(bt)_2(acac)$, suggesting a possible energy transfer from **NONP** and **NONM** to $Ir(bt)_2(acac)$, which can be confirmed by the emission spectra of $Ir(bt)_2(acac)$ doped in **NONP** and **NONM** dichloromethane solutions with different doped concentrations (Fig. S1). The triplet state lifetimes (τ) for two hosts are in millisecond scale at 40 K (Table 1, Fig. S2). Low-temperature PL measurement was detected at 40 K (Fig. 2) to calculate the triplet energies of the **NONP** and **NONM** as 2.71 and 2.73 eV, respectively (Table 1). These energies are higher than the triplet energy of the common yellow phosphorescent dopant $Ir(bt)_2(acac)$ (E_T = 2.2 eV) [14]. Hence, **NONP** and **NONM** can be appropriate hosts for $Ir(bt)_2(acac)$ and carriers can be well-confined in the emissive layers.

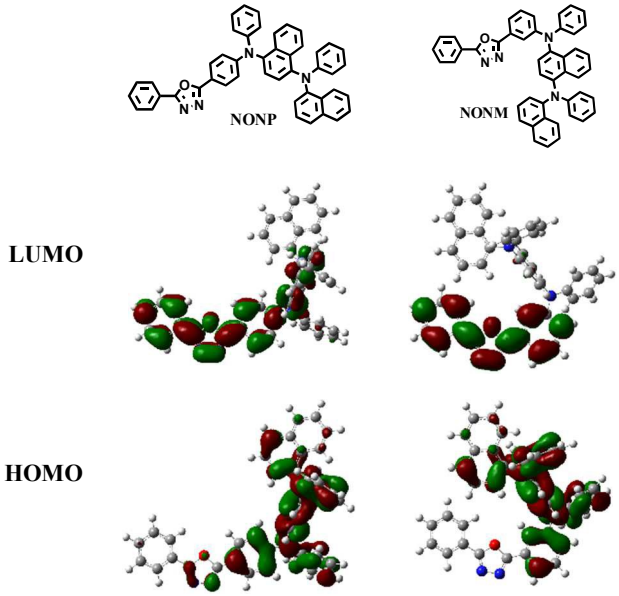

Fig. 3 Spatial distributions of the HOMO and LUMO levels for **NONP** and **NONM**.

To gain insight into the geometrical and electrical properties of the compounds, quantum chemistry calculation was performed using the TDDFT/B3LYP/6-31G(d**) method.[15] As shown in Fig. 3, their HOMOs (highest occupied molecular orbitals) are localized predominantly on the electron-rich **NPNA2** unit and the buffer unit of benzene attached to it, and the LUMOs (lowest unoccupied molecular orbitals) are localized predominantly on electron-deficient **OXD** fragments. And as minor different electronic properties, the photoluminescent features between two hosts were also similar.

Compared with the slightly overlap between HOMO and LUMO for **NONP**, **NONM** has almost complete separation of the HOMO and LUMO due to the steric effects in *meta*-linkage through benzene unit. Two host materials both have potential to show bipolar property, which is an important factor for enhancing the efficiency and lowering the operating voltage of PHOLEDs.[16]

Cyclic voltammetry (CV) was performed to study the electrochemical property of **NONP** and **NONM**. Fig. 4 shows that both compounds have two reversible reduction and oxidation behaviors, indicating a good electrochemical stability and their potential to have bipolar carrier-transporting property.[17] The HOMO energy levels of two compounds were calculated from onset potentials of oxidation as -5.27 and -5.25 eV for **NONP** and **NONM**, respectively, by comparing with ferrocene (Fc) (HOMO = -(E_{ox}+4.8)eV). The corresponding LUMO levels calculated from the HOMO values and the band gaps (which were estimated to be 2.94 and 2.95 eV from the edge of UV-Vis absorption) were found to be approximately -2.33 (**NONP**) and -2.30 eV (**NONM**), respectively. Thus, theoretically low holes and electrons injection barriers between the widely used hole-transporting layer (1,1-bis[4-(di-*p*-tolylamino)phenyl]cyclohexane (TAPC, -5.50/-2.0 eV)[18] or electron-transporting layer 1,3,5-tri(*m*-pyrid-3-yl-phenyl)benzene (TmPyPB, -6.68/-2.73 eV)[19] and hosts can be realized.

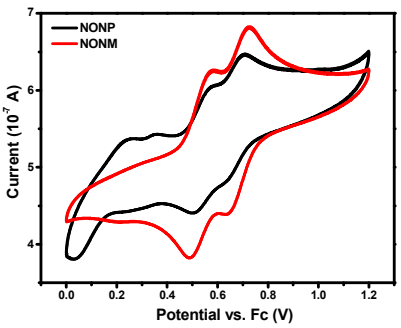

Fig. 4 Cyclic voltammograms of **NONP** and **NONM** in dichloromethane solution with 0.1 M $TBAPF_6$ as supporting electrolyte.

OLEDs performance

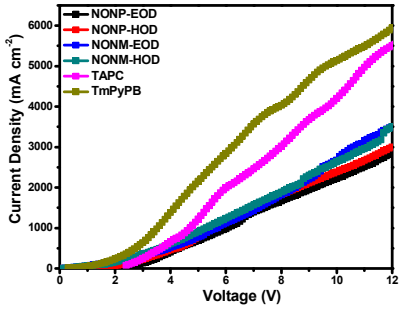

Fig. 5 Current density *versus* voltage for the hole-only (**HOD**) and the electron-only (**EOD**) devices.

The charge-transporting property of two compounds was investigated by fabricating hole-only and electron-only devices. The hole-only devices (**HODs**) have the configuration of ITO (indium tin oxide) / host (30 nm)/ TAPC (60 nm)/ Al (100 nm), while the electron-only devices (**EODs**) have the configuration of ITO/ TmPyPB (60 nm)/ host (30 nm)/ LiF (1 nm)/ Al (100 nm). The TAPC or TmPyPB layer was used to prevent electron- or hole-injection from cathode or anode, respectively. And we also fabricated the TAPC-only and TmPyPB-only devices. The current density *versus* the voltage curves for these devices are shown in Fig. 5. As the current densities of TAPC and TmPyPB are much larger than **HODs** and **EODs**, the effect of TAPC and TmPyPB on charge transport can be neglected. In **HODs** and **EODs**, both **NONP** and **NONM**-based devices showed smaller difference of current density between **HODs** and **EODs**. This indicates that the two compounds are capable of transporting holes and electrons and exhibit bipolar character by the introduction of the hole transport unit **NPNA2** and electron-drawing moiety **OXD**. The hole and electron current density of **NONM** was slightly higher than those of **NONP**, which indicates that **NONM** could show better performance than **NONP** in terms of charge transportation. This can be attributed to the asymmetric substitution at the *meta*-position which is an effective strategy for the design of high-performance bipolar host materials.[17]

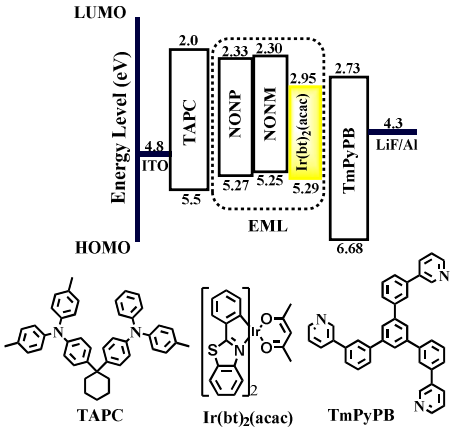

Fig. 6 Energy level diagram of yellow PHOLEDs and molecular structures of materials used.

The electroluminescence (EL) performance of the bipolar host materials **NONP** and **NONM** were evaluated with devices having the common structure ITO/ TAPC (40 nm)/ host: $Ir(bt)_2(acac)$ (15 wt%, 20 nm)/ TmPyPB (40 nm)/ LiF (1 nm)/ Al (100 nm). The molecule structures and energy level diagrams of the materials and devices are shown in Fig. 6. TAPC and TmPyPB were used as the hole- and electron-transporting layers, respectively. $Ir(bt)_2(acac)$ was used as the phosphor emitter with the optimized doping concentration of 15 wt%, which is a little higher than common yellow devices.[20] This is because more electrons were trapped

directly at the dopant molecules at higher doping level due to the low LUMO level of $Ir(bt)_2(acac)$, which provided an additional channel to transport electrons through hopping between the dopant sites.[21] Accordingly, higher dopant concentration such as 15 wt% improved the charge balance and energy transfer from host to guest.[22]

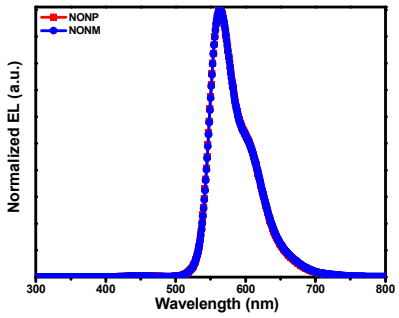

Fig. 7 EL spectra of **NONP**- and **NONM**-based yellow PHOLEDs.

The EL spectra of the **NONP-** and **NONM-**based yellow PHOLEDs showed a main peak at 562 nm and a slight shoulder peak appeared at 595 nm from $Ir(bt)_2(acac)$ (Fig. 7), and both the devices emit yellow light with Commission Internationale de l'Eclairage(CIE) color coordinates of (0.49, 0.51). This means that the host materials undergo highly efficient exothermic energy transfer from the host to dopant in the emitting layer upon electrical excitation. Additionally, no other emission bands were observed in the devices, which is partly due to the well-balanced charge density in the emission zone.[22]

As shown in Fig. 8 a, the current density-voltage-luminance (*J* - *V* - *L*) characteristic curves of the **NONP**- and **NONM**-based devices demonstrate the turn-on voltage is only 2.7 V. One important reason for such low turn-on voltage is the bipolar transporting property of the hosts. Another reason is the suitable HOMO and LUMO energy levels of two hosts, which better matches the work function of the hole-transporting layer TAPC and electron-transporting layer TmPyPB, and improves charge injection of the device. The current density of the yellow PHOLED with **NONM** as the host was higher than that of the yellow PHOLED with **NONP** as the host, which is in agreement with the current density - voltage curves of the **HODs** and **EODs** shown in Fig. 5.

All the devices show good performances for the emission in yellow region, better than our previous results using silane-based hole transport host materials.[9] Futhermore, the device by *para*-linked host **NONP** achieves a maximum current efficiency ($\eta_{c,max}$) of 43.2 cd A^{-1}, a maximum power efficiency ($\eta_{p,max}$) of 35.7 lm W^{-1} and a maximum external quantum efficiency (EQE) of 12.9% with a maximum luminance of 70156 cd m^{-2} at 11.7 V. In comparison, the device using *meta*-linked **NONM** as the host exhibits a slightly higher efficiencies with a $\eta_{c,max}$ of 44.4 cd A^{-1}, a $\eta_{p,max}$ of 35.9 lm W^{-1}, an EQE of 13.5% and a maximum brightness of 65737 cd m^{-2} at 10.1 V,which can be elucidated from the following two aspects. First, the compound **NONM** appears to have a better balance of electron- and hole-transporting properties than that of compound **NONP**, which may result in balanced charge densities and a broad distribution of recombination regions within the emitting layer. Second, the slightly higher triplet energy of **NONM** (2.73 eV) could more efficiently suppress adverse energy back-transfer from the $Ir(bt)_2(acac)$ to the host than that **NONP** (2.71 eV), consequently resulting in better performances. This also proved that the efficiencies were improved by only changing the position of the substituents.

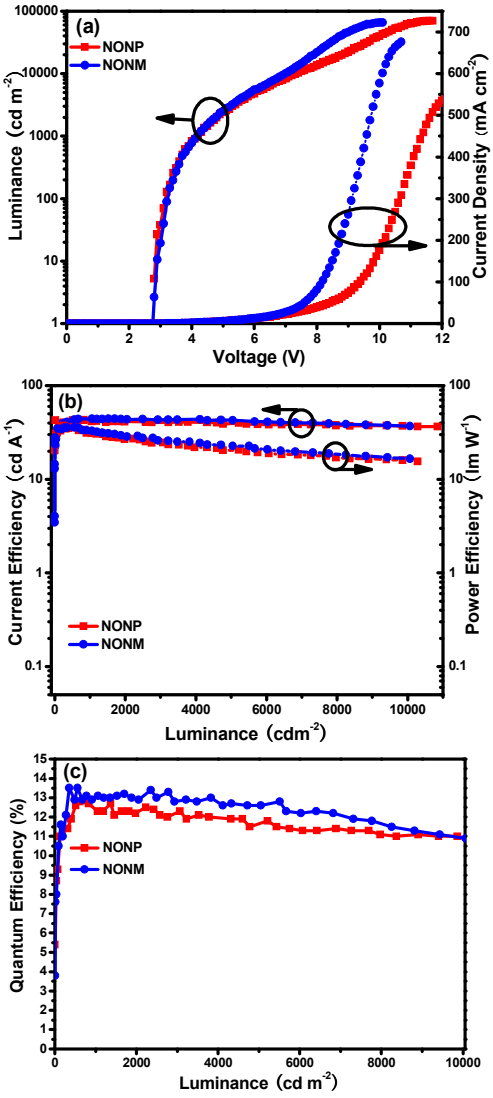

Fig. 8 (a). Current density-voltage-luminance (*J* - *V* - *L*); (b). current efficiency-luminance (η_c - *L*) and power efficiency-luminance (η_p - *L*); (c). external quantum efficiency - luminance (*EQE* - *L*) characteristics of the PHOLEDs with **NONP** and **NONM**.

It is worthy to mention that the current efficiency roll-off

ratios for both devices are mild. For example, at the luminance of 3000 cd m^{-2}, the current efficiency values of **NONP**- and **NONM**-based devices are still as high as 40.4 and 43.6 cd A^{-1}, respectively. This can be attributed to the balanced charge density and efficient exciton recombination in the broad area of the emitting zone.[23]

Conclusions

Two new bipolar materials, **NONP** and **NONM**, comprising hole-transporting unit N^1-(naphthalen-1-yl)-N^1,N^4-diphenylnaphthalene-1,4-diamine and electron-transporting moiety 1,3,4-oxadiazole were successfully synthesized. Two materials showed sufficient high triplet energy, good thermal ability and balanced charge mobility. Used as hosts for yellow PHOLEDs with low efficiency roll-off, the device bearing *meta*-linked **NONM** displayed performances with a maximum current efficiency of 44.4 cd A^{-1}, a maximum power efficiency of 35.9 lm W^{-1} and maximum external quantum efficiency of 13.5%, a maximum luminance of 70156 cd m^{-2}, a little higher than that of the *para*-linked host **NONP**-based device with a maximum current efficiency of 44.4 cd A^{-1}, a maximum power efficiency of 35.9 lm W^{-1} and maximum external quantum efficiency of 13.5%, a maximum brightness of 65737 cd m^{-2}. These results indicated that this work provided a way for designing ideal host materials for yellow PHOLEDs.

Table 2. Electroluminescence performances of the devices based on **NONP** and **NONM**.

Host	$V_{turn\text{-}on}$ [a]	L_{max} (voltage)[b]	$\eta_{c,max}$(luminance) [c]	$\eta_{c,L3000}$ [d]	$\eta_{p,max}$(luminance) [e]	EQE_{max} [f]	CIE [g]
	(V)	[cd m^{-2} (V)]	[cd A^{-1}(cd m^{-2})]	[cd A^{-1}]	[lm W^{-1}(cd m^{-2})]	[%]	[x,y]
NONP	2.7	70156 (11.7)	43.2 (612)	40.4	35.7 (612)	12.9	0.49, 0.51
NONM	2.7	65737 (10.1)	44.4 (1703)	43.6	35.9 (556)	13.5	0.49,0.51

[a] $V_{turn\text{-}on}$: Turn-on voltage recorded at a luminance of 1 cd m^{-2}; [b] L_{max}: maximum luminance; [c] $\eta_{c,max}$: maximum current efficiency; [d] $\eta_{c,L3000}$: current efficiency at 3000 cd m^{-2}; [e] $\eta_{p,max}$: maximum power efficiency; [f] EQE_{max}: maximum external quantum efficiency; [g] measured at 8 V.

Experimental

Materials and measurements.

^{1}H NMR and ^{13}C NMR spectra were measured on a Bruker AM 500 spectrometer. Mass spectra (MS) were obtained with MALDI-TOF (Bruker Daltonic Inc.). High resolution electrospray ionisation mass spectra (HR ESI-MS, Agilent 6540 UHD Accurate-Mass Q-TOF LC/MS) were recorded for the compounds. TGA and DSC measurements were carried out on STA 449F3 (NETZSCH) and 823e (METTLER), respectively. Absorption and emission spectra were measured on a Shimadzu UV-3100 and a Hitachi F-4600 luminescence spectrophotometer, respectively. The low temperature phosphorescence spectra were measured with an Edinburgh Instruments FLS-920 spectrophotometer at 40 K. Cyclic Volta metric experiments were carried out with an CHI 600E system (Chenhua, Shanghai) using three electrode cell assemblies in deaerated dichloromethane solution with tetrabutylammoniumperchlorate as supporting electrolyte at a scan rate of 100 mV s^{-1}. Each oxidation potential was calibrated with ferrocene as a reference.

OLEDs fabrication and measurement.

Organic chemicals used for OLEDs were generally purified by high-vacuum, gradient temperature sublimation. The devices were fabricated by vacuum deposition of the materials at 10^{-6} Torr onto a ITO glass substrate (a sheet resistance of 15 Ω square^{-1}) with a deposition rate of 1-2 Å s^{-1}. The phosphor and host were co-evaporated to form 20 nm emitting layer from two separate sources. The LiF and Al were deposited with deposition rates of 0.1 and 3 Å s^{-1}, respectively. The characteristics of the devices were measured with a computer controlled KEITHLEY 2400 source meter with a calibrated silicon diode in air without device encapsulation. The CIE coordinates were calculated using a testing program of the Spectra scan PR650 spectrophotometer.

Syntheses.

All reactions were performed under nitrogen. Solvents were carefully dried and distilled from appropriate drying agents prior to use for syntheses of ligands. **NPNA2** was synthesized according to our previous report.[9]

2-(4-Bromophenyl)-5-phenyl-1,3,4-oxadiazole. Benzoyl chloride (5 mmol, 0.70 g) was added dropwise to a solution of 4-bromobenzoyl hydrazine (5 mmol, 1.08 g) and triethylamine (5 mmol, 0.50 g) in chloroform (8 mL) at room temperature. The resulting mixture was stirred for 1 h and then filtered. The collected solid was washed with water and ethanol to give the product *N*-benzoyl-4-bromobenzohydrazide (1.51 g, yield: 95%). A mixture of *N*-benzoyl-4-bromobenzo-hydrazide (1.51g) and $POCl_3$ (15 mL) in a 100 mL flask was refluxed under nitrogen for 5 h. The excessive $POCl_3$ was then distilled out, and the residue was poured into water. The crude product was collected by filtration and purified by recrystallization from

chloroform/hexane to give white needlelike crystals (1.21 g, yield: 85%). ^{1}H NMR (500 MHz, $CDCl_3$) δ 8.18 – 8.16 (m, 1H), 8.16 (s, 1H), 8.04 (d, J = 8.5 Hz, 2H), 7.71 (d, J = 8.5 Hz, 2H), 7.57 (td, J = 8.7, 4.9 Hz, 3H). MALDI-TOF MS (FAB, *m/z*) calcd. for $C_{14}H_9BrN_2O$: 299.990. Found: 300.458 $[M]^+$.

2-(3-Bromophenyl)-5-phenyl-1,3,4-oxadiazole. 2-(3-Bromophenyl)-5-phenyl-1,3,4-oxadiazole was prepared according to the same procedure as compound 2-(4-bromophenyl)-5-phenyl-1,3,4-oxadiazole but 3-bromobenzoyl hydrazine instead of 4-bromobenzoyl hydrazine was used as a starting material. ^{1}H NMR (500 MHz, $CDCl_3$) δ 8.31 (d, J = 1.3 Hz, 1H), 8.20 – 8.15 (m, 2H), 8.12 (dd, J = 7.8, 0.9 Hz, 1H), 7.72 (dd, J = 8.0, 0.9 Hz, 1H), 7.61 – 7.55 (m, 3H), 7.45 (t, J = 7.9 Hz, 1H). MALDI-TOF MS (FAB, *m/z*) calcd. for $C_{14}H_9BrN_2O$: 299.990. Found: 300.479 $[M]^+$.

***N*^{1}-(Naphthalen-1-yl)-*N*^{1},*N*^{4}-diphenyl-*N*^{4}-(4-(5-phenyl-1,3,4-oxadiazol-2-yl)phenyl)naphthalene-1,4-diamine (NONP).** $Pd_2(dba)_3$ (0.09 g, 0.10 mmol), **NPNA2** (0.04 g, 1.0 mmol), Li^{t}BuO (0.32 g, 4.0 mmol) and 2-(4-bromophenyl)-5-phenyl-1,3,4-oxadiazole (0.36 g, 1.2 mmol) were added into a 50 mL two-neck flask. The flask was evacuated and backfilled with nitrogen. *O*-xylene (20 mL) and P^{t}Bu$_3$ (1.23 mL, 0.4 mmol, 10% in *n*-hexane) were injected. The mixture was heated at 140 °C for 48 h and extracted twice with CH_2Cl_2 at room temperature. The mixed organic solution was washed with brine and the solid obtained was purified with column chromatography on SiO_2 using ethyl acetate and petroleum ether (v : v = 1: 50) as eluant to afford yellowish solid **NONP** (67%). ^{1}H NMR (500 MHz, $CDCl_3$) δ 8.12 (ddd, J = 19.7, 16.7, 8.5 Hz, 4H), 7.95 (td, J = 13.6, 8.1 Hz, 4H), 7.75 (d, J = 8.3 Hz, 1H), 7.54 (dd, J = 10.9, 4.7 Hz, 3H), 7.50 (d, J = 7.1 Hz, 1H), 7.41 (ddd, J = 15.8, 12.2, 7.6 Hz, 4H), 7.35 – 7.30 (m, 4H), 7.21 – 7.16 (m, 3H), 7.14 – 7.09 (m, 2H), 7.03 (d, J = 8.9 Hz, 2H), 6.93 (t, J = 7.3 Hz, 2H), 6.80 (d, J = 8.0 Hz, 2H). ^{13}C NMR (126 MHz, $CDCl_3$) δ[ppm] 164.71, 163.91, 151.52, 150.35, 146.75, 144.68, 144.08, 139.44, 135.29, 132.48, 131.64, 131.42, 130.27, 129.55, 129.06, 129.02, 128.55, 128.16, 127.84, 126.93, 126.78, 126.65, 126.34, 126.13, 125.92, 125.28, 125.21, 125.13, 124.43, 124.32, 124.22, 124.08, 123.95, 120.99, 120.58, 119.04, 115.27. HR ESI-MS (*m/z*) calcd. for $C_{46}H_{32}N_4O$: 657.2649. Found: 657.2650 $[M+1]^+$.

***N*^{1}-(Naphthalen-1-yl)-*N*^{1},*N*^{4}-diphenyl-*N*^{4}-(3-(5-phenyl-1,3,4-oxadiazol-2-yl)phenyl)naphthalene-1,4-diamine (NONM).** Compound **NONM** was prepared according to the same procedure as compound **NONP** but 2-(3-bromophenyl)-5-phenyl-1,3,4-oxadiazole instead of 2-(4-bromophenyl)-5-phenyl-1,3,4-oxadiazole was used as a starting material with a yield of 60%. ^{1}H NMR (500 MHz, $CDCl_3$) δ 8.14 (d, J = 8.5 Hz, 1H), 8.10 (dd, J = 6.7, 1.6 Hz, 3H), 8.03 (d, J = 8.1 Hz, 1H), 7.91 (d, J = 8.4 Hz, 1H), 7.86 – 7.84 (m, 1H), 7.74 (d, J = 8.2 Hz, 1H), 7.69 (d, J = 7.7 Hz, 1H), 7.59 – 7.51 (m, 3H), 7.48 (d, J = 8.1 Hz, 2H), 7.43 – 7.30 (m, 7H), 7.19 – 7.09 (m, 6H), 7.04 (t, J = 7.3 Hz,2H), 6.91 (t, J = 7.3 Hz, 1H), 6.80 (d, J = 7.4 Hz, 2H). ^{13}C NMR (126 MHz, $CDCl_3$) δ[ppm] 150.37, 149.28, 147.68, 144.67, 143.68, 140.10, 135.26, 132.54, 131.66, 130.24, 129.96, 129.43, 129.04, 128.51, 127.65, 126.94, 126.76, 126.56, 126.30, 126.15, 126.08, 125.83, 125.27, 125.18, 125.08, 124.85, 124.60, 124.37, 124.22, 123.96, 122.78, 122.56, 120.84, 120.47, 119.71, 118.91. HR ESI-MS (*m/z*) calcd. for $C_{46}H_{32}N_4O$: 657.2649. Found: 657.2627 $[M+1]^+$.

Acknowledgements

This work was supported by the National Natural Science Foundation of China (21371093, 91433113), the Major State Basic Research Development Program (2011CB808704, 2013CB922101) and the Natural Science Foundation of Jiangsu Province (BK20130054)

Notes and references

State Key Laboratory of Coordination Chemistry, Collaborative Innovation Center of Advanced Microstructures, School of Chemistry and Chemical Engineering, Nanjing University, Nanjing 210093, P. R. China, e-mail: yxzheng@nju.edu.cn

1 E. Mondal, W. –Y. Hung, H. –C. Dai, H. –F. Chen, P. –Y. Hung and K. –T. Wong, *Tetrahedron*, 2014, **70**, 6328.

2 (*a*) F. -M. Hsu, C. -H. Chien, P. -I Shih and C. -F. Shu, *Chem. Mater.*, 2009, **21**, 1017; (*b*) M. A. Baldo, C. Adachi and S. R. Forrest, *Phys. Rev. B*, 2000, **62**, 10967; (*c*) X. Xu, X. Yang, J. Dang, G. Zhou, Y. Wu, H. Li and W.-Y. Wong, *Chem. Commun*., 2014, 50, 2473; (*d*) X. Yang, G. Zhou and W.-Y. Wong, *J. Mater. Chem. C*, 2014, 2, 1760.

3 (*a*) S. -J. Su, H. Sasabe, T. I. Takeda and J. Kido, *Chem. Mater.*, 2008, **20**, 1691; (*b*) B.H. Zhang, G. P. Tan, C. -S. Lam, B. Yao, C. -L. Ho, L. H. Liu, Z. Y. Xie, W. -Y. Wong, J. Q. Ding and L. X. Wang, *Adv. Mater.,* 2012, **24**, 1873.

4 M. Sudhakar, P. I. Djurovich, T. E. Hogen-Esch and M. E. Thompson, *J. Am. Chem. Soc.*, 2003, **125**, 7796.

5 (*a*) J. S. Swensen, E. Polikarpov, A. V. Ruden, L. Wang, L. S. Sapochak and A. B. Padmaperuma, *Adv. Mater.*, 2011, **21**, 3250; (*b*) K. Goushi, R. Kwong, J. J. Brown, H. Sasabe and C. Adachi, *J. Appl. Phys.*, 2004, **95**, 7798; (*c*) Q. Wang, I. W. H. Oswald, M. R. Perez, H. P. Jia, A. A. Shahub, Q. Q. Qiao, B. E. Gnade and M. A. Omary, *Adv. Funct. Mater.*, 2014, **24**, 4746; (*d*) Q. Wang, I. W. H. Oswald, M. R. Perez, H. P. Jia, B. E. Gnade and M. A. Omary, *Adv. Funct. Mater.*, 2013, **23**, 5420; (*f*) Q. Wang, I. W. H. Oswald, X. L. Yang, G. J. Zhou, H. P. Jia, Q. Q. Qiao, Y. H. Chen, J. Hoshikawa-Halbert and B. E. Gnade, *Adv. Mater.*, 2014, **26**, 8107.

6 (*a*) Y. T. Tao, C. L. Yang and J. G. Qin, *Chem. Soc. Rev.*, 2011, **40**, 2943; (*b*) Y. T. Tao, Q. Wang, C. L. Yang, Q. Wang, Z. Q. Zhang, T. T. Zou, J. G. Qin and D. G. Ma, *Angew. Chem. Int. Ed.*, 2008, **120**, 8224; (*c*) H. H. Chou and C. H. Cheng, *Adv. Mater.*, 2010, **22**, 2468; (*d*) S. L. Gong, Q. Fu, Q. Wang, C. L. Yang, C. Zhong, J. G. Qin and D. G. Ma, *Adv. Mater.*, 2011, **23**, 4956; (*e*) M. S. Lin, L. C. Chi, H. W. Chang, Y. H. Huang, K. C. Tien, C. C. Chen, C. H. Chang, C. C. Wu, A. Chaskar, S. H. Chou, H. C. Ting, K. T. Wong, Y. H. Liu and Y. Chi, *J. Mater. Chem.*, 2012, **22**, 870; (*f*) H. F. Chen, T. C. Wang, W. Y. Hung, H. C. Chiu, C. Yun and K. T. Wong, *J. Mater. Chem.*, 2012, **22**, 9658; (*g*) E. Mondal, W. Y. Hung, H. C. Dai and K. T. Wong, *Adv. Funct. Mater.*, 2013, **23**, 3096; (*h*) H. C. Ting, Y. M. Chen, H. W. You, W. Y. Hung, S. H. Lin, A. Chaskar, S. H. Chou, Y. Chi, R. H. Liu and K. T. Wong, *J. Mater. Chem.*, 2012, **22**, 8399; (*i*) H. F. Chen, T. C. Wang, S. W. Lin, W. Y. Hung, H. C. Dai, H. C. Chiu, K. T. Wong, M. H. Ho, T.

Y. Cho, C. W. Chen and C. C. Lee, *J. Mater. Chem.*, 2012, **22**, 15620; (*j*) H. F. Chen, L. C. Chi, W. Y. Hung, W. J. Chen, T. Y. Hwu, Y. H. Chen, S. H. Chou, E. Mondal, Y. H. Liu and K. T. Wong, *Org. Electron.*, 2012, **13**, 2671; (*k*) S. J. Su, C. Cai and J. Kido, *J. Mater. Chem.*, 2012, **22**, 3447.

7 F. Dumur and F. Goubard, *New J. Chem.*, 2014, **38**, 2204.

8 Y. -L. Liao, C. -Y. Lin, K. -T. Wong, T. -H. Hou, W. -Y. Hung, *Org. Lett.*, 2007, **9**, 4511.

9 S. Zhang, L. -S. Xue, Y. -M. Jing, X. Liu, G. -Z. Lu, X. Liang, H. -Y. Li, Y. -X. Zheng and J. -L. Zuo, *Dyes Pigm.*, 2015, **118**, 1.

10 S. –H. Cheng, S. –H. Chou, W. –Y. Hung, H. –W. You, Y. –M. Chen, A. Chaskar, Y. –H. Liu and K. –T. Wong, *Org. Electron.*, 2013, **14**, 1086.

11 T. Giridhar, W. Cho, Y. –H. Kim, T. –H. Han, T. –W. Lee and S. –H. Jin, *J. Mater. Chem. C*, 2014, **2**, 9398.

12 S. Zhang, Q. -L. Xu, Y. -M. Jing, X. Liu, G. -Z. Lu, X. Liang, Y. -X. Zheng, J. -L. Zuo, *RSC Advances*, 2015, **5**, 27235.

13 (*a*) X. Wei, J. Peng, J. Cheng, M. Xie, Z. Lu, C. Li and Y. Cao, *Adv. Funct. Mate.r*, 2007, **17**, 3319; (*b*) S. M. Chen, G. P. Tan, W. -Y. Wong and H. -S. Kwok, *Adv. Funct. Mater.*, 2011, **21**, 3785.

14 B. H. Zhang, G. P. Tan, C. -S. Lam, B. Yao, C. -L. Ho, L. H. Liu, Z. Y. Xie, W. -Y. Wong, J. Q. Ding and L. X. Wang, *Adv. Mater.*, 2012, **24**, 1873.

15 A. D. Becke, *J. Chem. Phys.,* 1993, **98**, 5648.

16 (*a*) C. Fan, F. Zhao, P. Gan, S. Yang, T. Liu, C. Zhong, D. Ma, J. Qin and C. Yang, *Chem. -Eur. J.*, 2012, **18**, 5510; (*b*) C. Han, Y. Zhao, H. Xu, J. Chen, Z. Deng, D. Ma, Q. Li and P. Yan, *Chem. -Eur. J.*, 2011, **17**, 5800.

17 (*a*) Y. T. Tao, Q. Wang, C. L. Yang, Q. Wang, Z. Q. Zhang, T. T. Zou, J. G. Qin and D. G Ma, *Angew. Chem. Int. Ed.*, 2008, **47**, 8104; (*b*) Y. -L. Liao, C. -Y. Lin, K. -T. Wong, T. -H. Hou and W. -Y. Hung, *Org. Lett.*, 2007, **9**, 4511; (*c*) Y. Shirota and H. Kageyama, *Chem. Rev.*, 2007, **107**, 953; (*d*) C. –J. Zheng, J. Ye, M. –F. Lo, M. –K. Fung, X. –M. Ou, X. –H. Zhang and C. –S. Lee, *Chem. Mater.*, 2012, **24**, 643.

18 G. Liaptsis and K. Meerholz, *Adv. Funct. Mater.*, 2013, **23**, 359.

19 J. -K. Bin, N. -S. Cho and J. -I. Hong, *Adv. Mater.*, 2012, **24**, 2911.

20 H. -F. Chen, T. -C. Wang, S. -W. Lin, W. -Y. Hung, H. -C. Dai, H. -C. Chiu, K. -T. Wong, M. -H. Ho, T. -Y. Cho, C. -W. Chen and C. -C. Lee, *J. Mater. Chem.*, 2012, **22**, 15620.

21 F. -M. Hsu, C. -H. Chien, P. -I. Shih and C. -F. Shu, *Chem. Mater.*, 2009, **21**, 1017.

22 S. Zhang, Q. –L. Xu, Y. –M. Jing, X. Liu, G. –Z. Lu, X. Liang, Y. –X. Zheng and J. –L. Zuo, *RSC Advances*, 2015, **5**, 27235.

23 M. J. Cho, S. J. Kim, S. H. Yoon, J. Shin, T. R. Hong, H. J. Kim, Y. H. Son, J. S. Kang, H. A. Um, T. W. Lee, J. –K. Bin, B. S. Lee, J. H. Yang, G. S. Chae, J. H. Kwon and D. H. Choi, *ACS Appl. Mater. Interfaces*, 2014, **6**, 19808.